2018 IEEE Conference on Control Technology and Applications (CCTA)
Copenhagen, Denmark, August 21-24, 2018

Accepted article

Discrete-time adaptive hysteresis filter for parallel computing and recursive identification of Preisach model

Michael Ruderman[1] and Dmitrii Rachinskii[2]

Abstract— **High-precision motion control systems, for instance deployed for micro- and nano-positioning, often use the smart-material based actuators such as piezoelectric and magnetostrictive stages. Those exhibit inherent hysteresis nonlinearities which are challenging to compensate without precise hysteresis modeling. Even if a suitable hysteresis modeling approach is available, its parameter identification, correspondingly adaptation, at normal operating conditions constitute an essential task for the overall control design. This paper uses the direct recursive identification method for the Preisach hysteresis model and describes the fast parallel-computing discrete-time algorithm for an adaptive hysteresis filter. The exponential convergence of errors is ensured up to a residual level proportional to the power of the measurement noise. We provide an explicit discrete-time formulation of the hysteresis filter and its online parameter adaptation. In addition to the theoretical analysis, we demonstrate the expected convergence of the estimation errors by using experimental data from a standard open-loop controlled piezoelectric actuator stage.**

I. Introduction

Hysteresis, as a quasi-static nonlinearity, appears in various piezoelectric, magnetostrictive, and other smart-actoric technologies as a factor aggravating their accurate control, for instance in micro- and nano-positioning [1]. Identification of parameters of the hysteresis at normal operating conditions is a challenging task for a model-based, or model-supported, control synthesis and tuning. The Preisach hysteresis model [2], [3] is one of the most powerful approaches to rate-independent hysteresis modeling, which has proved its worth in various engineering fields. An accurate identification of the Preisach hysteresis loops with the associated measure distribution on the Preisach plane, and a finite number of optimally chosen input-output experiments, have been proposed in [4]. In [5], the problem of hysteresis parameter identification with limited experimental data has been addressed by establishing links to regularization methods for the ill-posed problems. Similar developments can be found later in [6]. More recent attempts [7] develop a compressive sensing-based approach, while using a dedicated 'damped oscillation' input sequence in accord with the discretized Preisach model. Surprisingly, only a few recursive methods suitable for online Preisach model identification have been analyzed theoretically and proved with experiments, from which two different approaches [8] and [9] can be mentioned.

In this paper, we provide the fast parallel computing discrete-time algorithm for adaptive hysteresis filter using the direct recursive identification method proposed in [9]. The straightforward discrete-time formulation, including the adaptive scheme, is augmented by the convergence analysis in the presence of output noise – the case most significant for engineering practice. We demonstrate an example of the application involving measurements from a piezoelectric stage. Further, we analyze the residual errors, and show the proportionality between the output noise power and residual error norm of the Preisach measure distribution, which is in agreement with our analysis.

[1]M Ruderman is with Faculty of Engineering and Science, University of Agder, Norway, michael.ruderman@uia.no

[2]D Rachinskii is with Department of Mathematical Sciences, University of Texas at Dallas, USA, dmitry.rachinskiy@utdallas.edu

II. Discrete-Time Adaptive Hysteresis Filter

A. Hysteresis primitive (hysteron)

The Preisach hysteresis model [2], [3] is based on a weighted superposition of spatially distributed hysteresis primitives – hysterons, each one modeled by a non-ideal (delayed) two-points relay, see Fig. 1. The hysteron assumes

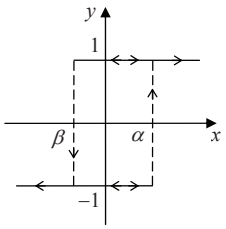

Fig. 1. Hysteresis primitive (hysteron).

either of two binary states $\{-1,+1\}$, while a discrete switching occurs at exceeding of the threshold values β and α, which are parameterizing the hysteron within the so-called Preisach half-plane $\alpha \geq \beta$. As long as an external input of the hysteron operator lies between the thresholds, i.e. $x \in (\beta,\alpha)$, the hysteron keeps its previous states, thus providing a local memory effect for the output value y. Recall that the local memory manifests itself through the map $\big(x(k),y(k-1)\big) \mapsto y(k)$, where $k \geq 0$ are the discrete (integer) time instants.

Following [10], the hysteresis primitive can be written in a closed analytic form which is particularly suitable for fast parallel computing of multiple hysterons building the Preisach model. Given the initial state

$$y(0) = \begin{cases} \chi(x(0)), & \text{if } x(0) \in (-\infty,\beta) \vee (\alpha,\infty), \\ [-1,+1]\,, & \text{otherwise,} \end{cases} \tag{1}$$

the hysteron state, correspondingly output, equation is

$$y(k) = \min\Big[\chi(x(k)-\beta), \max\big[y(k-1), \chi(x(k)-\alpha)\big]\Big]. \tag{2}$$

Further we define the signum operator as

$$\chi\big(\sigma(k)\big) = \begin{cases} 1, & \text{if } \sigma(k) \geq 0, \\ -1, & \text{otherwise,} \end{cases} \tag{3}$$

for $\big(\sigma(k) - \sigma(k-1)\big) > 0$, and as

$$\chi\big(\sigma(k)\big) = \begin{cases} 1, & \text{if } \sigma(k) > 0, \\ -1, & \text{otherwise,} \end{cases} \tag{4}$$

for $\big(\sigma(k) - \sigma(k-1)\big) < 0$. Note that the direction-dependent case differences (3) and (4) are necessary in order to ensure that the hysteron is always switching at the thresholds, even if a time-varying input remains exactly at the threshold value.

B. Recursive identification of Preisach hysteresis

The discretized Preisach hysteresis model can be seen as a weighted superposition of a finite number L of hysteron operators $y_i = h_i(p)[x]$, with the input x and output y according to (2). Recall that $L = (N^2 + N)/2$ when N is the discretization level of the Preisach plane. Each hysteron is weighted by $R_i > 0$ and assigned to the pair $p_i = (\alpha_i, \beta_i)$ which determines the hysteron's location within the Preisach half-plane $P = \{p = (\alpha, \beta) : \alpha \geq \beta\}$. Recall that the overall weight distribution $R(p_i), \forall\, i = 1, \ldots, L$ over the Preisach half-plane determines the shape of input-output hysteresis loops, and is to be identified for the given hysteresis system. Given the above notations, the discrete-time output of the Preisach hysteresis model is

$$z(k) = \sum_{i=1}^{L} R_i h_i(p)\big[x(k)\big]. \tag{5}$$

Furthermore, one can show that if $P^+ \subseteq P$ is a subset of those hysterons whose instantaneous state is $+1$, then the hysteresis model output can be also written as

$$z = \sum_{P^+} R_i(p). \tag{6}$$

The direct recursive identification algorithm, proposed in [9] and analyzed in detail in [11], aims to determine the Preisach distribution $R(p)$, using the estimate $\hat{R}(p)$ that converges monotonically to $R(p)$ with the progressing discrete time k. We denote those subset of hysterons which switch on, i.e. change their state from -1 to $+1$ at the time step k, by $S^+(k) = P^+(k) \backslash P^+(k-1)$. Similarly, the subset of hysterons which switch off, i.e. change their state from $+1$ to -1, is denoted by $S^-(k) = P^+(k-1) \backslash P^+(k)$. The corresponding number of switching hysterons is $A = \dim(S)$. The identification algorithm uses the differential output error $e(k) = z(k) - z(k-1) - \hat{z}(k) + \hat{z}(k-1)$, where z represents the hysteresis system output and $\hat{z}$ is its model-based estimate, i.e. the output of the adaptive hysteresis filter under identification. Based on the introduced subsets of switching hysterons and (6), one can show that

$$e(k) = \sum_{S^+(k)} \big(R_i - \hat{R}_i\big) - \sum_{S^-(k)} \big(R_i - \hat{R}_i\big). \tag{7}$$

The direct recursive identification algorithm updates the weight of those hysterons that have $p_i = (\alpha_i, \beta_i)$ in the switching region

$$S(k) = S^+(k) \cup S^-(k).$$

The update rate is determined according to, cf. [9], by

$$\hat{R}_i(k) = \hat{R}_i(k-1) + r(k), \quad p_i \in S(k)$$

with

$$r(k) = \begin{cases} e(k)A^{-1}(k) & \text{if } p \in S^+(k), \\ -e(k)A^{-1}(k) & \text{if } p \in S^-(k), \end{cases}, \tag{8}$$

where $A(k)$ is the number of nodes in the switching region. At the same time, $\hat{R}_i(k) = \hat{R}_i(k-1)$ for $p_i \in P \setminus S(k)$. Note that the update rate is evaluated once at each discrete time step, and applies to all the hysterons belonging to the switching subset, cf. further with sections II-C, II-D.

The Euclidian norm of the Preisach distribution estimation error can be written as

$$\big\|\hat{R}(k) - R\big\| = \Big(\sum_{i=1}^{L} \big(\hat{R}_i(k) - R_i\big)^2\Big)^{1/2}. \tag{9}$$

In [11] it has been shown that (9) is monotonically decreasing for stochastic input processes and almost surely converges to zero exponentially, i.e. $\big\|\hat{R}(k) - R\big\| \leq C \exp(-\lambda k)$ for some positive constants C and λ, in absence of the measurement noise. In presence of the measurement noise $\big\|\hat{R}(k) - R\big\| \to \mathrm{const}$, and that also exponentially with k, while the residual constant depends on the noise power as will be analyzed further in section III.

C. Adaptation of hysteron weights

Assuming the recursive identification algorithm given above in section II-B, the single hysteron weight is adapted at the fractional time instant $k + 0.5$, i.e. between the current and next state of the discrete-time filter. This is required due to implementation-related synchronization between two successive discrete time steps, i.e. k and $k+1$, since at the next time step the already updated hysteresis model output has to be compared with that from the system. Further we note that this requires either an auxiliary (internal) triggering clock, i.e. impulse generator, or the double sampling rate compared to the rate initially assumed for the hysteresis filter without weight adaptation. Such implementation issues have, however, no impact on the proposed algorithm and, as less relevant, will not be discussed in detail here.

It is evident that for the given hysteron states, the differential quantity

$$s(k) = 0.5\big|y(k) - y(k-1)\big| \tag{10}$$

provides the binary variable $s(k) \in \{0, 1\}$ that indicates whether the hysteron has been switching or not. Therefore, the normalized area of switching region is given by

$$A(k) = \sum_{i=1}^{L} s_i(k). \tag{11}$$

This is fed into the update law (8). Finally, the corresponding hysteron weight is adapted by

$$\hat{R}_i(k+0.5) = \hat{R}_i(k) + r(k)s(k). \tag{12}$$

D. Structure of adaptive filter

The block diagram of the adaptive hysteresis filter is shown in Fig. 2. The unknown static hysteresis plant is driven by an exogenous input $x(k)$, which is assumed to be available and used for hysteresis identification. Recall that the static, i.e. rate-independent, hysteresis is invariant to affine time transformations. That means the system response is independent of the spectral characteristics of the input signal, and solely the sequence of local input extrema determines the memory state of hysteresis. Here it is worth to emphasize that the rate-independent hysteresis remains a widely accepted and reasonable approach for describing the hysteresis phenomena in functional materials, even if various attempts of merging the hysteresis with residual, not necessarily nonlinear, system dynamics have been made.

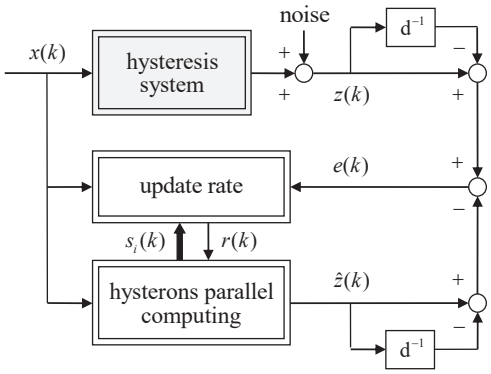

Fig. 2. Block diagram of the adaptive hysteresis filter.

The available hysteresis output is subject to the measurement noise for which only assumptions about the power can be made, as will be addressed in section III. Both the output of hysteresis system and the output of the adaptive filter we design are feed through the discrete-time backward shift operator d^{-1}, also denoted as single time delay, so that the differential output error $e(k)$ is obtained. The error is used for computing the update rate of the switching hysterons, while their parallel computation provides the output of the adaptive hysteresis filter $\hat{z}(k)$.

III. Convergence in presence of noise

In the presence of measurement, i.e. sensor, noise $n(k)$ the hysteresis system output, cf. Fig. 2, results in

$$z(k) = \sum_{P^+(k)} R_i(p) + n(k). \tag{13}$$

As a standard sensor assumption, each sample of $n(k)$ has a normal distribution with zero mean and variance W, and the samples are i.i.d. (independent and identically distributed) that is a Gaussian white noise. W can be directly estimated as the standard average power of the measurement noise

$$W = \frac{1}{K}\sum_{k=1}^{K} n^2(k), \quad \text{with} \quad K \to \infty. \tag{14}$$

With each point $p_i = (\alpha_i, \beta_i)$ on the Preisach half-plane P, we associate the collection of other points

$$\Delta_i = \{p_j = (\alpha_j, \beta_j) \in P : \beta_i \le \beta_j \le \alpha_j \le \alpha_i\},$$

which can be called a (discretized) "triangle". We will say that the input series creates all the possible triangles over a time interval $k = k_\ell, k_\ell + 1, k_\ell + 2, ..., k_{\ell+1}$ if

- for each node $p_i \in P$, there is a time instant k with $k_\ell \le k \le k_{\ell+1}$ such that the switching region $S(k)$ is the triangle Δ_i;
- all relays are switched off at the moments k_ℓ, $k_{\ell+1}$

(the 2nd condition is technical and included for convenience).

Let us denote the error of the estimate of the weight distribution at the k-th time step by $E(k) = \hat{R}(k) - R$. With this notation, from the update rule one obtains the relation

$$\|E(k+1)\|^2 = \|E(k)\|^2 - \frac{1}{A(k)}\Big(\sum_{S(k)} E_i(k)\Big)^2 + \frac{\nu^2(k)}{A(k)} \tag{15}$$

for every k, where

$$\nu(k) = n(k+1) - n(k).$$

A further analysis shows that if the input creates all the possible triangles over the time interval between two moments k_ℓ and $k_{\ell+1}$, then there is at least one moment k within this time interval, such that

$$\Big(\sum_{S(k)} E_i(k)\Big)^2 \ge C(T_\ell, N)\|E(k_\ell)\|^2 - \frac{D(T_\ell, N)}{T_\ell}\sum_{k=k_\ell+1}^{k_{\ell+1}} \nu^2(k), \tag{16}$$

where

$$T_\ell = k_{\ell+1} - k_\ell$$

and the coefficients $C(T_\ell, N)$, $D(T_\ell, N)$ satisfy

$$0 < C(T_\ell, N) < 1, \qquad D(T_\ell, N) > 0.$$

The coefficient $C(T_\ell, N)$ decreases with T_ℓ and N, while the coefficient $D(T_\ell, N)$ increases with T_ℓ and N. These coefficients can be estimated explicitly as shown below.

Relations (15) and (16) imply that

$$\|E(k_{\ell+1})\|^2 \le q(T_\ell)\|E(k_\ell)\|^2 + \frac{B(T_\ell, N)}{T_\ell}\sum_{k=k_\ell+1}^{k_{\ell+1}} \nu^2(k) \tag{17}$$

with

$$q(T_\ell, N) = 1 - C(T_\ell, N), \quad B(T_\ell, N) \le D(T_\ell, N) + T_\ell. \tag{18}$$

Denoting by $\langle\cdot\rangle$ the expected value of a random variable, and taking into account that $\langle\nu^2(k)\rangle = 2W$, from (17) we obtain

$$\big\langle\|E(k_{\ell+1})\|^2\big\rangle \le q(T_\ell, N)\big\langle\|E(k_\ell)\|^2\big\rangle + 2B(T_\ell, N)\,W. \tag{19}$$

Now, assume that there is an infinite increasing sequence of time moments $0 = k_0 < k_1 < \cdots < k_\ell < \cdots$ such that an input $x(k)$ creates all the possible triangles over each time interval $k_\ell \le k \le k_{\ell+1}$. (17) and (19) can be used to estimate $E(k)$ for various classes of such inputs. In particular, assume that the sequence $T_\ell = k_{\ell+1} - k_\ell$ is bounded:

$$T_\ell \le T, \quad \ell = 0, 1, 2, \ldots$$

Since both $q(T,N)$, $B(T,N)$ increase with T, (19) implies

$$\big\langle \|E(k_{\ell+1})\|^2 \big\rangle \le q(T,N) \big\langle \|E(k_\ell)\|^2 \big\rangle + 2B(T,N)\, W$$

for each ℓ. This leads to the estimate

$$\big\langle \|E(k_\ell)\|^2 \big\rangle \le q^\ell(T,N)\|E(0)\|^2 + \frac{2B(T,N)}{1-q(T,N)}\, W. \quad (20)$$

Here $q(T,N) = 1 - C(T,N) < 1$, cf. with (18). Hence, the effect of initial error $E(0)$ on the error $E(k_\ell)$ exponentially decays with time. In particular, for large k_ℓ one obtains

$$\limsup_{\ell\to\infty} \big\langle \|E(k_\ell)\|^2 \big\rangle \le 2\, \frac{B(T,N)}{C(T,N)}\, W. \quad (21)$$

That is, an upper bound of the variance of the residual error (after a sufficient number of iterations) is proportional to the the measurement noise power.

We note that the iterations of the mean $\big\langle E(k) \big\rangle$ follow the update rule with zero (averaged out) noise, and hence $\big\langle E(k) \big\rangle$ exponentially converges to zero as shown in [11].

Next, assume that the input is a random process. For simplicity, assume that the times T_ℓ that it generates are i.i.d. (possibly unbounded) random variables, which are also independent of the measurement noise. Considering the average over the realizations of the input, from (19) one obtains the estimates

$$\big\langle \|E(k_\ell)\|^2 \big\rangle \le \big(1 - \langle C(T_\ell,N)\rangle\big)^\ell \|E(0)\|^2 + \frac{2\langle B(T_\ell,N)\rangle}{\langle C(T_\ell,N)\rangle}\, W, \quad (22)$$

$$\limsup_{\ell\to\infty} \big\langle \|E(k_\ell)\|^2 \big\rangle \le 2\, \frac{\langle B(T_\ell,N)\rangle}{\langle C(T_\ell,N)\rangle}\, W, \quad (23)$$

which are similar to (20), (21) but now contain the expected values of the random variables $B(T_\ell,N)$, $C(T_\ell,N)$. Hence, again, the effect of the initial error exponentially vanishes, and an upper bound of the variance of the residual error is proportional to the measurement noise power.

Relations (21), (23) suggest that the variance of the residual error $\langle \|E_{res}\|^2 \rangle$ is proportional to the measurement noise power W. Indeed, in the next section we show this proportionality for a set of experimental data (Fig. 8) and evaluate the coefficient of proportionality numerically. This coefficient can also be estimated analytically. In particular, for $C(T,N)$, $D(T,N)$ in (16), we obtained the estimates

$$C(T,N) \ge \frac{1}{16N(NT+2)^2}, \quad D(T,N) \le T^2N^2 \quad (24)$$

which, when combined with (18), (21), lead to the estimate

$$\frac{\langle \|E_{res}\|^2 \rangle}{W} \le 2\, \frac{\langle B(T,N)\rangle}{C(T,N)} \le 32NT(NT+2)^2(TN^2+1) \quad (25)$$

for the ratio of $\langle \|E_{res}\|^2 \rangle$ and W. A similar estimate follows from (20), (21). However, these estimates are too conservative for practical use. Deriving more accurate practical estimates for the coefficient of proportionality between $\langle \|E_{res}\|^2 \rangle$ and W will be the subject of future work.

IV. Practical Example

A. Piezoelectric setup

The implemented adaptive discrete-time hysteresis filter (cf. Fig. 2) has been evaluated on the experimental data collected from a standard piezoelectric stage with one translational degree of freedom. For more details on the system hardware configuration we refer to [12], [13].

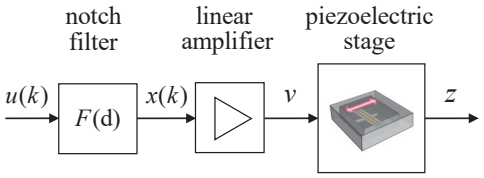

Fig. 3. Principal structure of experimental setup.

The principal structure of the experimental setup is schematically shown in Fig. 3. The power-amplified input voltage v drives the piezoelectric stage, from which the relative displacement, i.e. stroke, is measured by means of the linear encoder with a high-resolution of 1.22 nm/pulse. In order to eliminate the high-frequent resonant dynamics of the piezoelectric stage, the control input signal $u(k)$ is fed through the 4th-order notch filter. The latter is designed so as to suppress two most pronounced resonance peaks, and is based on the accurate measurement of the frequency response function. The determined discrete-time transfer function of the notch filter, in terms of the discrete shift operator d, is

$$F(\mathrm{d}) = \frac{0.430\mathrm{d}^4 - 1.409\mathrm{d}^3 + 1.987\mathrm{d}^2 - 1.385\mathrm{d} + 0.416}{\mathrm{d}^4 - 2.174\mathrm{d}^3 + 1.752\mathrm{d}^2 - 0.620\mathrm{d} + 0.081}. \quad (26)$$

The system sampling rate is 5 kHz. The frequency characteristics of the designed notch filter are shown in Fig. 4, together with the measured frequency response function (FRF) and the identified transfer function of a linear system approximation; an accurate match is clearly visible.

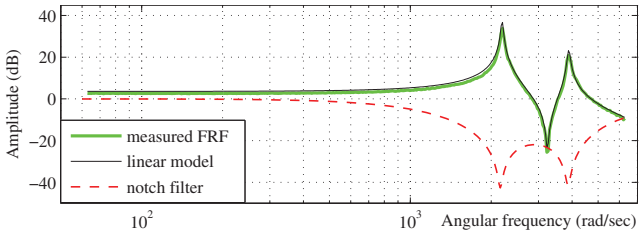

Fig. 4. Bode diagram of the measured system frequency response function, identified linear model, and designed notch filter.

A long-term input sequence has been generated as a standard Bernoulli process for the input voltage range between 0 V and 75 V. The carrier frequency of the input

process has been selected at 10 Hz, that is quite below the resonant dynamics of the piezoelectric stage, cf. with Fig. 4. Further, we note that the sharp corners at the input reversals are equally smoothed by the notch filter so that no transient oscillating disturbances occur in the measured stroke $z(k)$. Under such conditions, the residual input-output system behavior can be seen as quasi-static and, therefore, justifies the system approximation by a rate-independent hysteresis. An example of the measured input-output data is shown in Fig. 5. Note that the Bernoulli input sequence

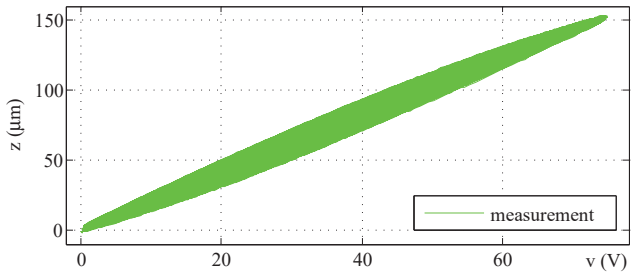

Fig. 5. Measured input-output hysteresis of the piezoelectric stage.

creates a large number of the closed (minor) hysteresis loops, so that a sufficiently large k can be faithfully assumed, cf. section III.

B. Recursive identification

The designed discrete-time adaptive hysteresis filter, cf. section II, has been evaluated on the input-output hysteresis data recorded from experiments. First, the total number of the hysterons has been set to $L = 703$ that corresponds to $N = 37$. Further, we note that a slightly reduced sampling rate of 2 kHz has been assumed. This was conditional by the

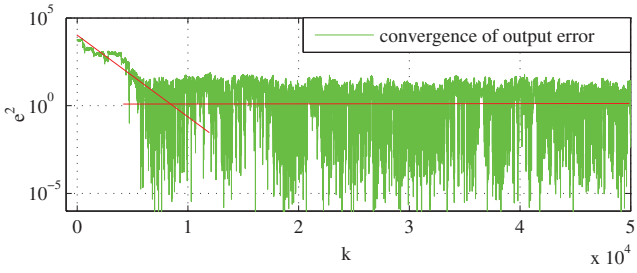

Fig. 6. Squared hysteresis output error of recursive identification.

implementation constraints of the available hardware. The Preisach distribution under evaluation has been uniformly initialized as $\hat{R}(k{=}0)$ = 1e–9. Since the true Preisach distribution of the system is not available, only the output estimation error can be assessed. The squared hysteresis output error $e^2(k)$ is shown logarithmically in Fig. 6 as a function of k. Two linear asymptotes (in red) indicate that the output error is (roughly exponentially) decreasing first, before starting to fluctuate at a residual level for larger k. Despite a highly irregular oscillating pattern of e^2, between 10^{-5} and 10^{1}, it can be recognized that the residual error of the recursive hysteresis identification remains close to constant on average. Neither convergence nor divergence occurs with a further increasing k, cf. Fig. 6 for $k > 10^4$.

C. Residual error analysis

While the sensor noise associated with the high-resolution (1.22 nm/pulse) encoder is relatively low, compared to the operation stroke range (cf. Fig. 5), and can be neglected therefore, the output measurement noise due to the discretization and quantization should be closer investigated and taken into account. It is also worth noting that the piezoelectric stage is subject to the process noise as well. However, this remains unconsidered as evident from (13). The most obvious sources of the process noise are the inherent creeping effects in the piezoelectric structures, see e.g. [14], [15], mechanical micro-shifts and misalignments of the stage and sensor, thermal and temporal relaxations, and others.

For the Preisach hysteresis system, the discretization and quantization noise appear due to an input quantization into N levels, with the corresponding quantization step

$$\delta x = \big(\max(x) - \min(x)\big)/N.$$

That means the output z is switching, correspondingly sampled, only upon reaching quantization levels of the input. Obviously the maximal increment

$$I = \max \frac{\partial z}{\partial x}, \tag{27}$$

over the entire hysteresis data is crucial for the output sampling. Given the hysteresis measurements, the I-value can be easily identified on either of both vertices of the major loop – due to the congruence property of the hysteresis [3] and convex and concave curvature of the increasing, correspondingly decreasing, hysteresis branches, cf. Fig. 5. From the measured hysteresis loops, $I = 2.53$ has been determined. Consequently, the upper bound of the output quantization step is estimated as

$$Z_q = I\,\delta x(N). \tag{28}$$

The effect of discretization and quantization is demonstrated in Fig. 7 on the measured and model-computed hysteresis output, from the same recursive identification experiment as shown in section IV-B. It is evident that

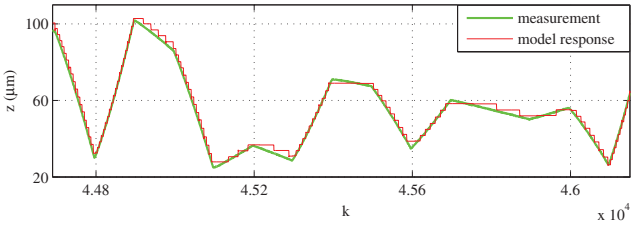

Fig. 7. Time frame of the recursive identification, measurement versus model with $N = 37$, with the visible discretization and quantization effect.

the output quantization levels can occur reciprocal to the measured output, since the sampling of both (measurement and model) is governed by the N-quantization of the input and is, therefore, of a rather stochastic nature.

Using the standard measure for the quantization noise power [16], i.e. $\delta^2/12$ where δ is the quantization step, we can assume an upper bound for the average power of the measurement noise as

$$W \approx \frac{I^2(\delta x)^2}{12}. \tag{29}$$

Since only the output error quantity is available from the identification experiment, we are to derive an auxiliary error norm that should be equivalent to the error norm $\|E\|^2$ of the estimated Preisach distribution. The averaged residual output error is obtained from the identification experiments by

$$\langle e \rangle = \Big(\frac{1}{M-m} \sum_{k=m}^{M} e^2(k) \Big)^{1/2}. \tag{30}$$

Note that the residual error interval $[m = 1e4, \dots, M = 5e4]$ has been assigned according to the observed convergence of the hysteresis output error, cf. Fig. 6. Due to the fact that all hysterons contribute simultaneously to e, and assuming $\hat{R}_i$ converges to its true value (up to the impact of the noise) $\forall\, i = 1, \dots, L$ and $k > m$, one can write

$$\langle \|E_{res}\|^2 \rangle \approx \langle \|E(k > m)\| \rangle = \Big((\langle e \rangle / L)^2 L \Big)^{1/2}. \tag{31}$$

In order to evaluate the above assumptions on the error norm, and assess the convergence bound in presence of noise, cf. section III, we consider the adaptive hysteresis filter with different discretizations of the Preisach plane $N = \{75, 37, 19, 13, 9\}$. The identification experiments executed for all five hysteresis models are similar to the case $N = 37$ described in section IV-B. The average norm of the residual estimation error and the average power of the measurement (quantization) noise, computed by (31) and (29) correspondingly, are plotted against each other in Fig. 8. An auxiliary

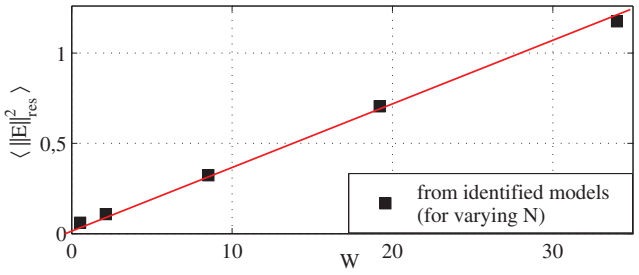

Fig. 8. Average norm of the residual estimation error as function of the average power quantization noise for $N = \{75, 37, 19, 13, 9\}$.

linear asymptote is also depicted (by red line), for a better comparison. One can see that the evaluated average error norm and the noise power are clearly proportional, which argues in favor of the analysis provided in section III.

V. Conclusions

The discrete-time adaptive hysteresis filter has been proposed for a fast parallel-computing and recursive identification of the rate-independent hysteresis. The algorithm is applicable to the smart-material-based actuators, for instance deployed for micro- and nano-positioning, where the hysteresis nonlinearity in the input channel should be compensated for linearizing system far as possible. We showed that the fast parallel computation and adaptation of the hysteresis primitives – hysterons – is possible in the real-time setting. We also analyzed the convergence of the direct recursive algorithm [9], [11] in the presence of inherent measurement noise. We showed that the variance of the Preisach weight distribution error decreases until it becomes proportional to the measurement noise power after a sufficient number of iterations. An experimental example, with input-output data from a standard piezoelectric stage, was shown in favor of the developed adaptive hysteresis filter and associated analysis.

Acknowledgments

D. Rachinskii acknowledges the support of NSF through grant DMS-1413223.

References

[1] A. J. Fleming and Y. K. Yong, "An ultrathin monolithic XY nanopositioning stage constructed from a single sheet of piezoelectric material," *IEEE/ASME Transactions on Mechatronics*, vol. 22, no. 6, pp. 2611–2618, 2017.

[2] F. Preisach, "Ueber die magnetische Nachwirkung," *Zeitschrift Physik (in German)*, vol. 94, pp. 277–302, 1935.

[3] I. D. Mayergoyz, *Mathematical models of hysteresis and their application*, 2nd ed. Amsterdam, Netherlands: Elsevier, 2003.

[4] K.-H. Hoffmann, J. Sprekels, and A. Visintin, "Identification of hysteresis loops," *Journal of Computational Physics*, vol. 78, no. 1, pp. 215–230, 1988.

[5] R. V. Iyer and M. E. Shirley, "Hysteresis parameter identification with limited experimental data," *IEEE Transactions on magnetics*, vol. 40, no. 5, pp. 3227–3239, 2004.

[6] M. Ruderman and T. Bertram, "Identification of soft magnetic bh characteristics using discrete dynamic preisach model and single measured hysteresis loop," *IEEE Transactions on Magnetics*, vol. 48, no. 4, pp. 1281–1284, 2012.

[7] J. Zhang, D. Torres, N. Sepúlveda, and X. Tan, "A compressive sensing-based approach for preisach hysteresis model identification," *Smart Materials and Structures*, vol. 25, no. 7, p. 075008, 2016.

[8] X. Tan and J. S. Baras, "Adaptive identification and control of hysteresis in smart materials," *IEEE Transactions on Automatic Control*, vol. 50, no. 6, pp. 827–839, 2005.

[9] M. Ruderman, "Direct recursive identification of the Preisach hysteresis density function," *Journal of Magnetism and Magnetic Materials*, vol. 348, pp. 22–26, 2013.

[10] M. Ruderman, "Computationally efficient formulation of relay operator for preisach hysteresis modeling," *IEEE Transactions on Magnetics*, vol. 51, no. 12, pp. 1–4, 2015.

[11] D. Rachinskiy and M. Ruderman, "Convergence of direct recursive algorithm for identification of Preisach hysteresis model with stochastic input," *SIAM Journal on Applied Mathematics*, vol. 76, no. 4, pp. 1270–1295, 2016.

[12] K. Seki, M. Ruderman, and M. Iwasaki, "Modeling and compensation for hysteresis properties in piezoelectric actuators," in *IEEE 13th Int. Workshop on Advanced Motion Control*, 2014, pp. 687–692.

[13] M. Ruderman and D. Rachinskii, "Online identification of piezoelectric hysteresis by direct recursive algorithm of Preisach model," in *IEEE International Conference on Mechatronics*, 2015, pp. 296–299.

[14] D. Croft, G. Shed, and S. Devasia, "Creep, hysteresis, and vibration compensation for piezoactuators: atomic force microscopy application," *Journal of Dynamic Systems, Measurement, and Control*, vol. 123, no. 1, pp. 35–43, 2001.

[15] K. Kuhnen and P. Krejci, "Compensation of complex hysteresis and creep effects in piezoelectrically actuated systemsa new preisach modeling approach," *IEEE Transactions on Automatic Control*, vol. 54, no. 3, pp. 537–550, 2009.

[16] B. Widrow and I. Kollár, "Quantization noise," *Cambridge University Press*, vol. 2, p. 5, 2008.